Sensors and Materials, Vol. 35, No. 7 (2023) 2637–2652
MYU Tokyo

S & M 3345

A Maximum Power Tracker for Photovoltaic Module Arrays Based on the Improved Perturbation and Observation Method

Thi Thanh Truc Bau and Kuei-Hsiang Chao*

Department of Electrical Engineering, National Chin-Yi University of Technology,
No. 57, Sec. 2, Zhongshan Rd., Taiping Dist., Taichung 41170, Taiwan

(Received February 9, 2023; accepted June 26, 2023)

Keywords: photovoltaic module array, maximum power point tracking, improved perturbation and observation method, voltage and current sensors, power–voltage characteristic curve, dynamic response, steady-state performance

In this paper, we propose a method based on improved perturbation and observation (I-P&O), which when used in conjunction with voltage and current sensors, enables the maximum power point tracking (MPPT) of the photovoltaic module array (PVMA), thereby increasing the power generation performance of the PVMA. The change in the maximum power output of the PVMA with varying sunlight intensities and temperature differences leads to a prolonged tracking time if the traditional perturbation and observation (P&O) method with small step-size tracking and a fixed value were adopted to find the maximum power point (MPP). Conversely, the adoption of a large step-size and a fixed value, even though the tracking speed is improved, causes a high amplitude oscillation around the point when tracked to the MPP, reducing the overall output power of the PVMA. Thus, an I-P&O method is proposed to solve this problem and to increase the output power of the PVMA. First, we set the initial voltage of the MPPT to 0.8-fold the voltage V_{mp} of the MPP for the PVMA under standard test conditions. At the same time, we auto-adjust the tracking step-size according to the slope value of the P–V characteristic curve for the PVMA. Then, we use 62050H-600S, a programmable DC power supply manufactured by Chroma ATE Inc., to simulate the output characteristics of a 5-series and 2-parallel PVMA, followed by tracking its MPP by the traditional P&O and I-P&O methods. Finally, from the experimental results, we proved that the proposed I-P&O method yields both a better tracking dynamic response and steady-state performance under different sunlight and temperature conditions.

1. Introduction

A photovoltaic power generation system is mainly composed of a photovoltaic module array (PVMA), power conditioner, and transmission and distribution system, wherein the power conditioner is also capable of tracking the maximum power point (MPP).[1–4] Because the output power of the PVMA varies on the basis of the insolation intensity and temperature, the PVMA

*Corresponding author: e-mail: chaokh@ncut.edu.tw
https://doi.org/10.18494/SAM4353

ISSN 0914-4935

should be controlled by the MPP tracker to ensure that the maximum power is delivered by the PVMA regardless of the insolation intensity or temperature.

A corresponding power–voltage (P–V) characteristic curve is generated by the PVMA on the basis of the ambient temperature and sunlight intensity, and the commonly used traditional maximum power point tracking (MPPT) techniques include the voltage feedback method, constant voltage method,[5] power feedback method,[6] perturbation and observation (P&O) method,[7] and incremental conductance (INC) method.[8] The voltage feedback method allows PVMA to work at the MPP by adjusting the output voltage of the PVMA. Its structure is simple and does not need complex calculations; however, since the method requires finding the voltage at the MPP in advance for the PVMA under a certain temperature and sunlight intensity, if the weather changes too quickly, this method will be unable to quickly and accurately track to the MPP. Furthermore, when the photovoltaic system ages or malfunctions, the voltage of its MPP changes and thus requires revisions be made to the parameters before tracking to the MPP.

The constant voltage method uses the measured voltage at the MPP of the PVMA under different temperature and sunlight intensity as the reference value, and adjusts the output voltage of the PVMA under different temperature and sunlight intensity so that it matches the reference value for achieving the maximum power tracking. Therefore, this method is easy to implement, highly reliable, easy to control, and highly stable. However, it lacks precision, and when weather conditions change considerably, the system is unable to track to the new MPP.

The power feedback method is similar to the voltage feedback method, except that its control method is more complex, where the rate of change of the output power to the output voltage $\mathrm{d}P/\mathrm{d}V$ is used as the judgment logic. When $\mathrm{d}P/\mathrm{d}V = 0$, it means that it has tracked to the MPP, but the chances of the system working at slope zero of the P–V curve is extremely low. Moreover, the structure of the power feedback method is more complex than that of the voltage feedback method, and the sensors within the circuit are also unable to make very precise measurements. However, there is less energy loss, and thus the overall efficiency is higher than that of the voltage feedback method.

The P&O method is used to make perturbations with minor voltage increments or decrements while measuring the output power; if the power increases, then we continue to adjust the voltage in the same direction. Conversely, if the power decreases, then we adjust the voltage in the opposite direction. The structure of the P&O method is simple, requires few parameters, and is easier to implement; it is also the most commonly used type of traditional tracking method. However, when tracked to the MPP by this method, because the system has tracked continuously, output power oscillates around the two sides of the MPP.

The INC method is derived from the power feedback method, where $\mathrm{d}P/\mathrm{d}V = 0$ is used as the condition for judging the system working at MPP. It is then derived into $\mathrm{d}I/\mathrm{d}V = -I/V$ to be used as the condition for judging the system working at MPP, in which $G_s = -I/V$ is static conductance and $G_d = \mathrm{d}I/\mathrm{d}V$ is dynamic conductance. By comparing the values of G_d and G_s, the location of the present working point to the left or right side of the MPP can be found. Although the INC method can improve the tracking accuracy and dynamic response of the P&O method in changing weather, the choice of the perturbation amount affects the overall tracking efficiency. If the value of the perturbation amount is set too large, the tracking speed will be high, but it can

easily cause the oscillation value under the steady-state to become too large. Conversely, if the value of the perturbation amount is set too small, the tracking speed will decrease, but the oscillation value under the steady-state will become smaller.

On the basis of the above advantages and disadvantages of the traditional MPPT techniques, the P&O method was chosen for this study to carry out the tracking of the MPP for the PVMA for the following reasons: few parameters, simple structure, easy-to-understand principles, and ease of control. Meanwhile, the traditional P&O method is used in this study as the basis to develop an improved perturbation and observation (I-P&O) method and to allow the characteristic curve of the PVMA to change according to the sunlight intensity and temperature, so that when a different output P–V characteristic curve is generated, its MPP tracker can achieve a better tracking speed response and steady-state performance.

2. MPPT Structure for PVMA

The PVMA developed in this study uses the Kyocera KS20 photovoltaic module (PVM), a PVM manufactured by the Japanese company Kyocera Co.,[9] with specifications as listed in Table 1. The current-voltage (I–V) and P–V characteristic curves of the Kyocera KS20 PVM under sunlight intensities of 1000 and 500 W/m^2 are shown in Fig. 1.

Table 1
Specifications of Kyocera KS20 PVM.

Open-circuit voltage V_{oc} (V)	21.5
Short-circuit current I_{sc} (A)	1.24
Voltage at MPP V_{mp} (V)	16.9
Current at MPP I_{mp} (A)	1.2
Maximum power P_{mp} (W)	20.28

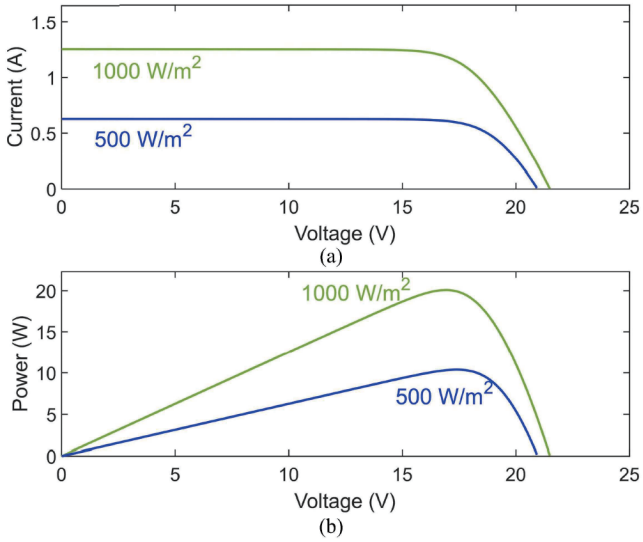

Fig. 1. (Color online) (a) I–V and (b) P–V characteristic curves of PVM under sunlight intensities of 1000 and 500 W/m^2.

Figure 2 shows the MPPT structure proposed in this study, among which the two subsystems include the (1) boost converter circuit and (2) I-P&O method. When carrying out the test, the voltage and current of the PVMA are fed back through the differential amplifier, and the digital signal processor TMS320F2809 is used to implement the I-P&O principle to control the switch conduction and cut-off time and to proceed to the MPPT of the PVMA.

3. Boost Converter Design

Figure 3 shows the circuit architecture of the boost converter,[10] in which its circuit structure is composed of the power switch, fast diode, energy-storage inductor, and filter capacitor. The power switch conductance and cut-off can be controlled through pulse width modulation control signals. The following five hypothesis need to be made before analyzing the circuit: (1) the circuit is being operated under steady-state; (2) the switch cycle is defined as T, the switch conduction time as DT, and the switch cut-off time as $(1-D)T$, for which, D is the duty cycle defined as $D \triangleq t_{on} / T$ and t_{on} is the switch conduction time within a cycle; (3) the inductor current is operated under the continuous conduction mode; (4) the capacitor value is extremely large so that the output voltage V_o is fixed; and (5) the circuit components are all ideal components.

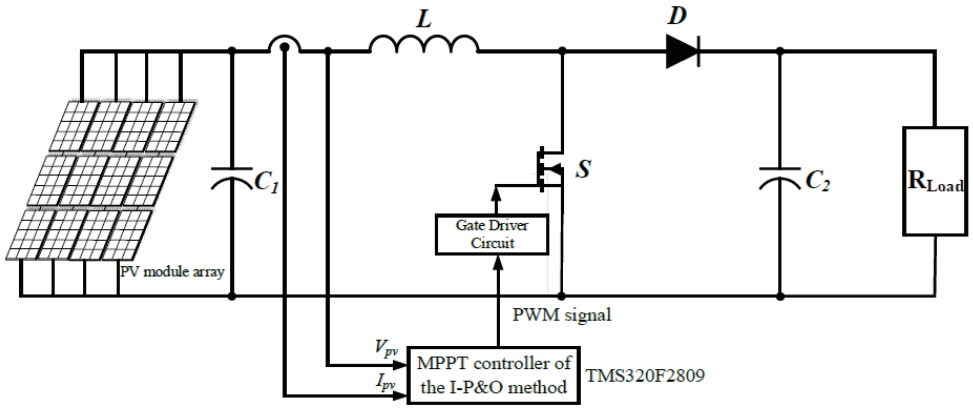

Fig. 2. Structural diagram of MPPT system for the proposed I-P&O method.

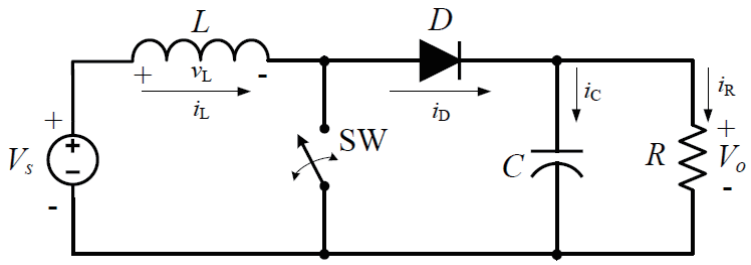

Fig. 3. Circuit architecture of boost converter.

When the switch SW is turned on, the diode (*D*) cuts off as a result of reverse bias. The equivalent circuit is shown in Fig. 4. At this time, the path of the current loop is composed of the voltage source (V_s), inductor (*L*), and switch (SW). Thus, the Eq. (1) can be derived from the Kirchhoff circuit law.

$$v_L = V_s = L\frac{di_L}{dt} \text{ or } \frac{di_L}{dt} = \frac{V_s}{L} \tag{1}$$

Since the rate of change of the inductor current is a positive value, when the switch is conducted, the inductor current increases linearly, and during the switch conduction period, the variation value of its inductor current is

$$\frac{\Delta i_L}{\Delta t} = \frac{\Delta i_L}{DT} = \frac{V_s}{L}. \tag{2}$$

From Eq. (2), the variation value of inductor current can be derived as

$$\left(\Delta i_L\right)_{closed} = \frac{V_s DT}{L}. \tag{3}$$

When the switch (SW) changes from conduction to cut-off, it can be derived from Lenz's law that the inductor current cannot change instantly, so the inductor induces a negative voltage, enabling the diode (*D*) to be in forward bias and form a loop with the inductor. Its equivalent circuit is shown in Fig. 5, and the voltage at the two terminals of the inductor at this time is

$$v_L = V_s - V_o = L\frac{di_L}{dt} \text{ or } \frac{di_L}{dt} = \frac{V_s - V_o}{L}. \tag{4}$$

Since the rate of change of the inductor current is a negative value, when the switch is cut off, the inductor current decreases linearly, and during the switch cut-off period, the variation value of its inductor current is

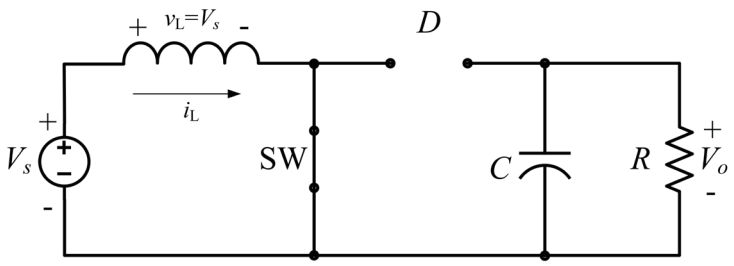

Fig. 4. Equivalent circuit when boost converter switch SW is conducted.

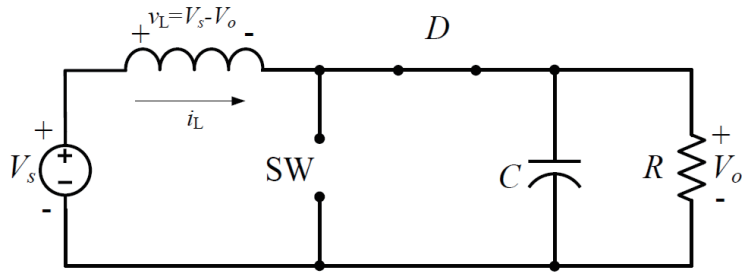

Fig. 5. Equivalent circuit when boost converter switch SW is cut off.

$$\frac{\Delta i_L}{\Delta t} = \frac{\Delta i_L}{(1-D)T} = \frac{V_s - V_o}{L}. \tag{5}$$

From Eq. (5), the variation value of its inductor current can be derived as

$$(\Delta i_L)_{open} = \frac{(V_s - V_o)(1-D)T}{L}. \tag{6}$$

Under steady-state operation, since the net change of the inductor current is zero, the following is derived.

$$(\Delta i_L)_{closed} + (\Delta i_L)_{open} = 0 \tag{7}$$

$$\frac{V_s DT}{L} + \frac{(V_s - V_o)(1-D)T}{L} = 0 \tag{8}$$

$$V_s DT + (V_s - V_o)(1-D)T = 0 \tag{9}$$

$$V_o = \frac{V_s}{1-D} \tag{10}$$

When $0 \le D \le 1$, $V_s \le V_o \le \infty$ is derived, this converter is called the boost converter.

When the boost converter is operating at high switching frequencies, the volumes of the energy storage inductor and filter capacitor can be shrunk. Therefore, the switching frequency of 25 kHz was selected for the boost converter in this study. Based upon design, the component specifications[10] for the boost converter are listed in Table 2.

Table 2
Component specifications for boost converter.

Components	Specifications
Filter capacitor C_1	Capacitance value 220 μF
	Withstand voltage 400 V
Filter capacitor C_2	Capacitance value 470 μF
	Withstand voltage 500 V
Energy storage inductor L	Inductance value 1.66 mH
	Withstand current 7.5 A
Fast diode D Diode IQBE60E60A1	Withstand voltage 600 V
	Withstand current 60 A
Power switch-MOSFET IRF460	Withstand voltage 500 V
	Withstand current 20 A

4. Proposed P&O Method

The traditional P&O method is the most commonly used among the traditional MPPT methods; its structure is simple and requires few parameters. The traditional P&O method compares the output power before and after the perturbation by increasing or decreasing the output voltage of the PVMA in a fixed cycle. If the output power increases after the perturbation, then we continue to perturb in the same direction. Otherwise, we perturb in the opposite direction. If the output voltage for the PVMA needs to be increased, then we reduce the duty cycle of the converter. Conversely, if the output voltage needs to be decreased, then we increase the duty cycle of the converter until it tracks to the MPP. Then, we generate an oscillation around the left and right sides of the MPP. Figure 6 shows the flow chart of the traditional P&O method being applied to the MPPT for the PVMA.

4.1 P&O method with fixed initial tracking voltage

Although the traditional P&O method is the most commonly used traditional tracking method, there is no significant difference in the tracking time between the traditional P&O method and other traditional tracking methods. Therefore, on the basis of the traditional P&O method, we propose to set the fixed initial tracking voltage V_{st} to 0.8-fold the voltage V_{mp} for the PVMA at MPP, that is, $V_{st} = 0.8V_{mp}$. Only one extra step is involved in the tracking process, but the tracking time is improved, and when the tracking time is shortened, the power generation efficiency of the photovoltaic power generation system is increased.

4.2 P&O method with both fixed initial tracking voltage and step-size adjustment

As the traditional P&O has a long tracking time, and the tracking oscillates near the MPP when tracked to the MPP, and although the P&O method with fixed initial tracking voltage can shorten the tracking time, an oscillation of large amplitude near the MPP cannot be avoided. This leads to power loss, thereby reducing the power generation efficiency. If a smaller step size is used to carry out the MPPT, even though oscillation in large amplitude near the maximum

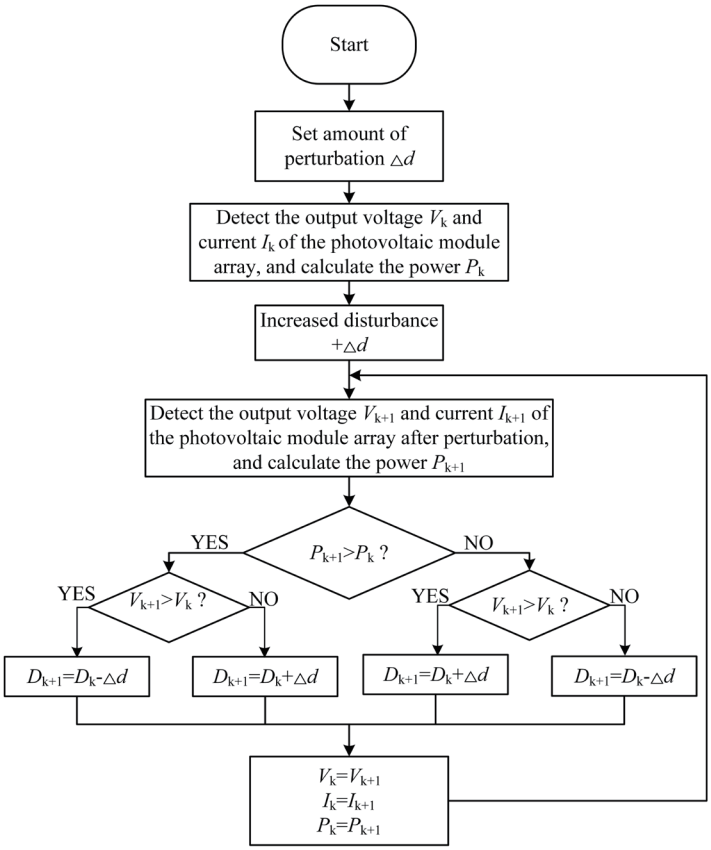

Fig. 6. Control flow chart of traditional P&O method.

power can be avoided, it lengthens the tracking time, thereby reducing the power generation performance. Therefore, to enhance the steady-state performance of the system, reduce the oscillation amplitude, and at the same time shorten the tracking time of the MPP, in addition to proposing a fixed initial tracking voltage, a method of making adjustments to the perturbation amount according to the work point is also proposed in this paper.[11,12] Since the traditional P&O method has already measured the output voltage and output power of the PVMA, these two parameters can be used to calculate the slope of the *P–V* characteristic curve using Eq. (11).

$$m_{k+1} = \frac{P_{k+1} - P_k}{V_{k+1} - V_k} \tag{11}$$

Besides setting the fixed initial tracking voltage to 0.8-fold the MPP voltage V_{mp} for the PVMA under standard test conditions, the perturbation amount Δd of the duty cycle for the converter is also adjusted at the same time using Eq. (12).

$$\Delta d_{k+1} = 5 \times 10^{-3} * \left| m_{k+1} \right| \tag{12}$$

From Eq. (12), it can be seen that the amount of perturbation is proportional to the slope, indicating that the closer to the MPP, the closer to zero for the slope of the *P–V* characteristic curve, and the amount of perturbation Δd also becomes closer to zero. Thus, when tracking to near the MPP, since the slope of the *P–V* characteristic curve approaches zero, the perturbation amount at this time also approaches zero, thereby increasing the tracking steady-state performance and enhancing the power generation efficiency of the PVMA. Figure 7 shows the diagram of the amount of change between the slope of the *P–V* characteristic curve and power for the PVMA.

5. Experimental Results

Figure 8 shows the *I–V* and *P–V* characteristic curves[13,14] obtained using a 5-series and 2-parallel array that is composed of the Kyocera KS20 PVM under sunlight intensities of 1000 and 500 W/m^2.

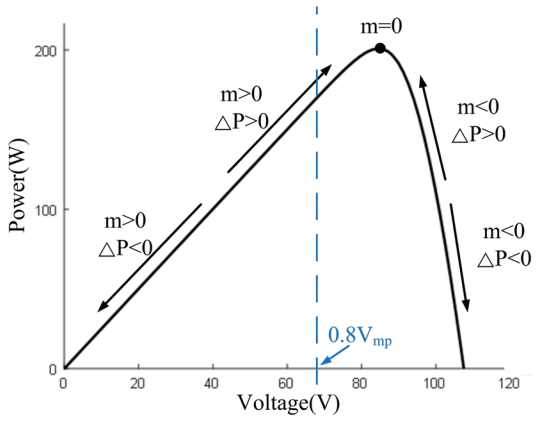

Fig. 7. (Color online) Diagram of the amount of change between the slope of the *P–V* characteristic curve and power for the PVMA.

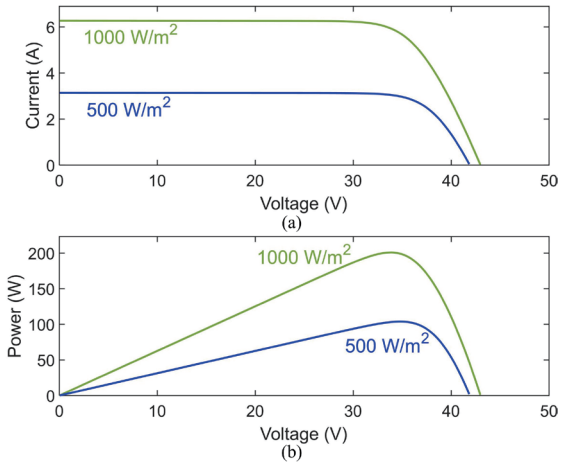

Fig. 8. (Color online) (a) *I–V* and (b) *P–V* characteristic curves of the 5-series and 2-parallel PVMA.

First, we created a photovoltaic power generation system with the boost converter[15] combined with the 5-series and 2-parallel PVMA to carry out the tracking of the MPP. Then, a programmable DC power supply (62050H-600S)[16] produced by Chroma ATE Inc. was used in this study to simulate the output characteristics of a 5-series and 2-parallel PVMA, followed by testing the MPPT by three different methods. Figures 9 and 10 show the resultant test waveforms of the *I–V* and *P–V* characteristic curves using the 5-series and 2-parallel PVMA under sunlight intensities of 1000 and 500 W/m^2, respectively. The actual circuit to perform the MPPT is obtained with Altium designer software[17] to complete the configuration of the wiring and components; the actual appearance of the circuit is shown in Fig. 11.

We proceeded to test the MPPT by the traditional P&O method. Figures 12 to 14 show the actual test results by applying the traditional P&O method and I-P&O methods with fixed initial tracking voltage and with both fixed initial tracking voltage together with tracking step-size adjustment under a sunlight intensity of 1000 W/m^2 and a temperature of 25 °C. Figures 15 to 17 show the actual test results of applying the traditional P&O method and I-P&O methods with fixed initial tracking voltage and with both fixed initial tracking voltage together with step-size adjustment under a sunlight intensity of 500 W/m^2 and a temperature of 25 °C.

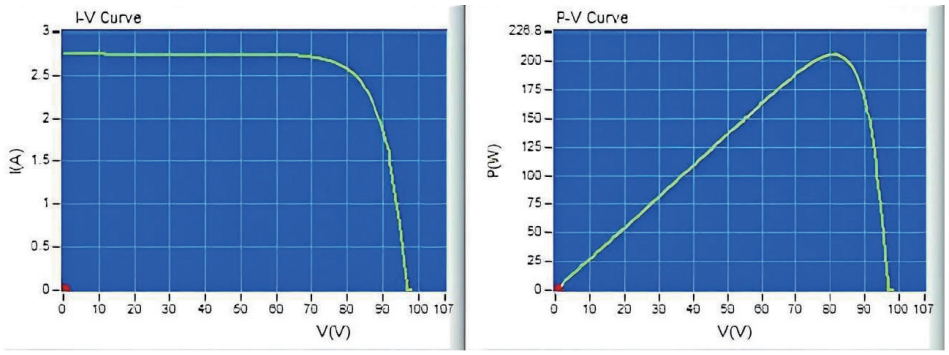

Fig. 9. (Color online) Tested *I–V* and *P–V* output characteristic curves of the 5-series and 2-parallel PVMA simulator under a sunlight intensity of 1000 W/m^2.

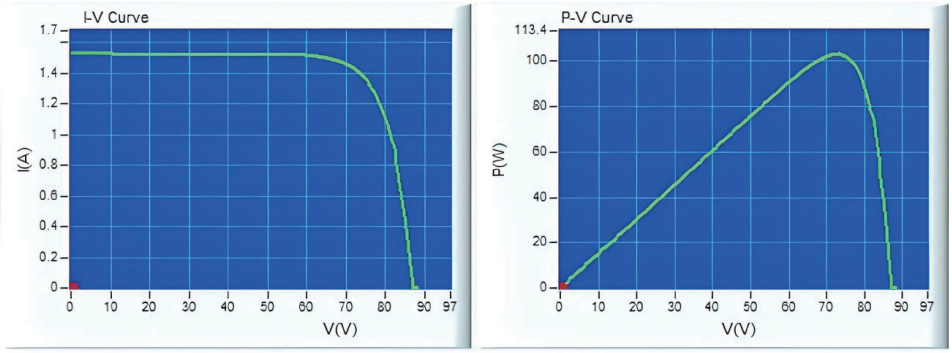

Fig. 10. (Color online) Tested *I–V* and *P–V* output characteristic curves of the 5-series and 2-parallel PVMA simulator under a sunlight intensity of 500 W/m^2.

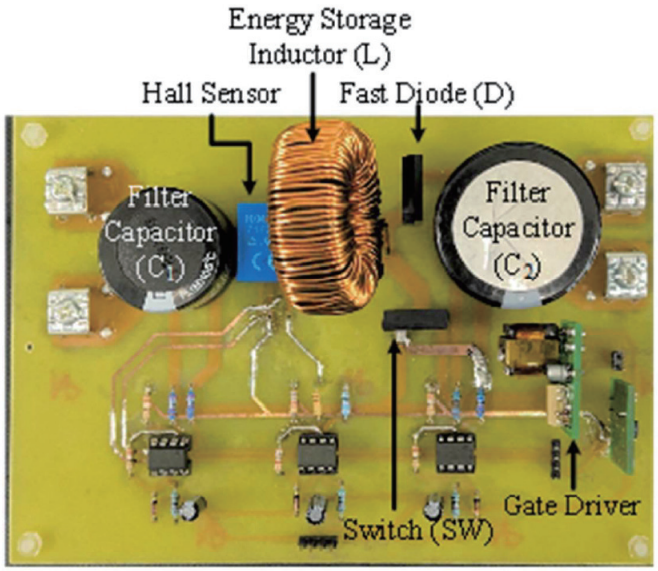

Fig. 11. (Color online) Appearance of actual circuit.

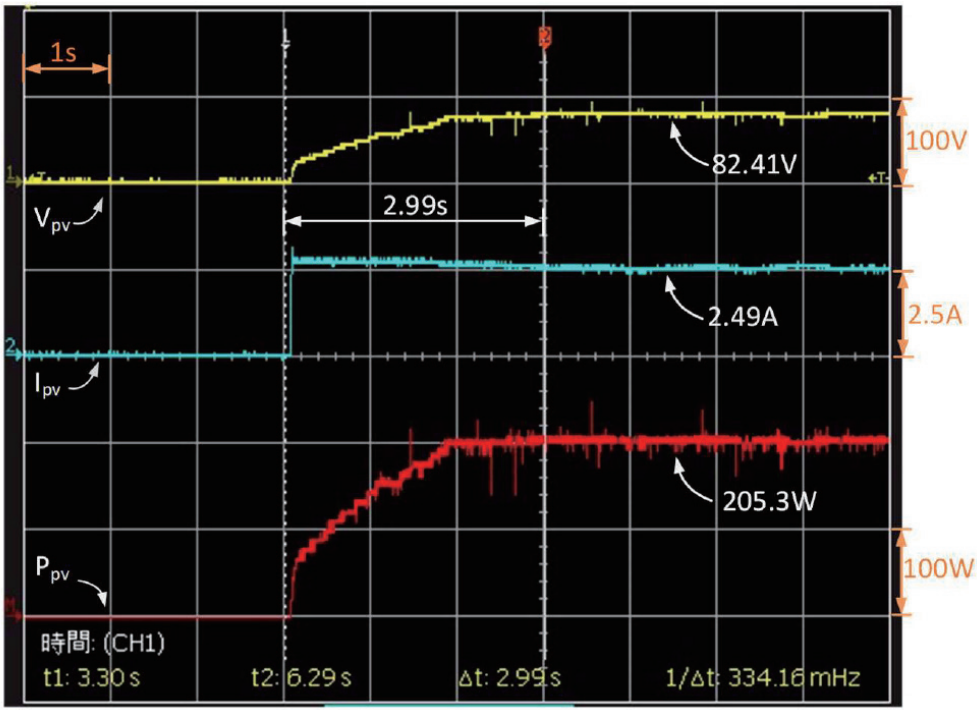

Fig. 12. (Color online) Actual test result of MPPT using the traditional P&O method under a sunlight intensity of 1000 W/m^2 and a temperature of 25 °C.

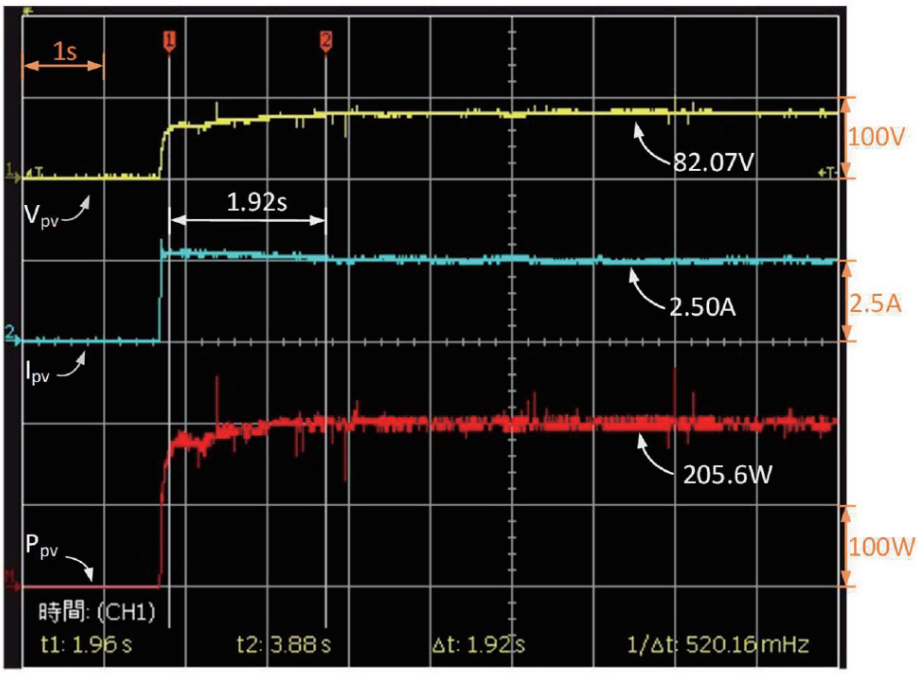

Fig. 13. (Color online) Actual test result of MPPT using the I-P&O method with fixed initial tracking voltage under a sunlight intensity of 1000 W/m^2 and a temperature of 25 °C.

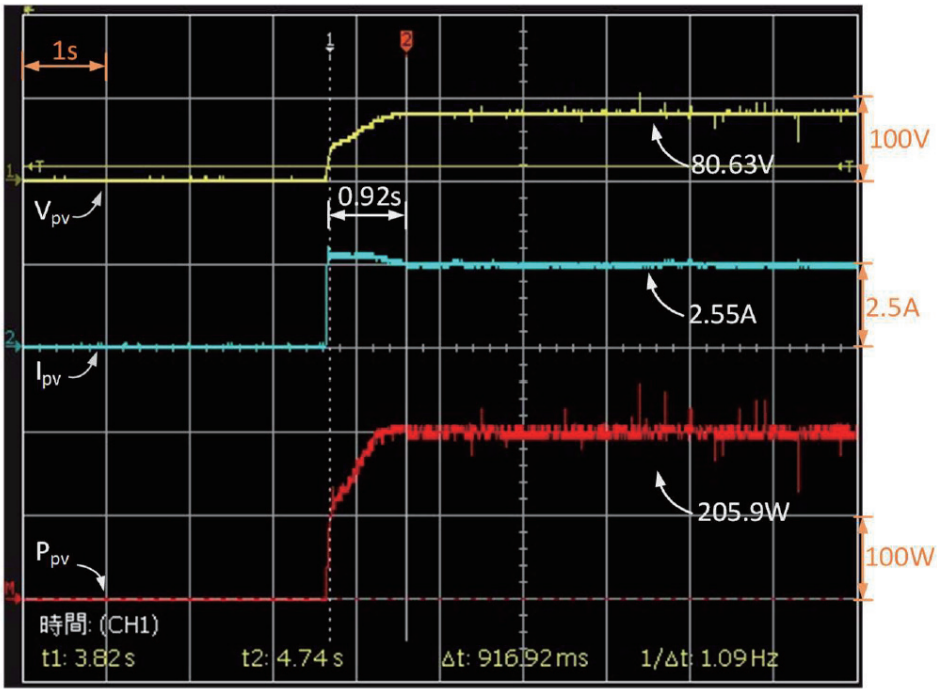

Fig. 14. (Color online) Actual test results of MPPT using the I-P&O method with both fixed initial tracking voltages and step-size adjustment under a sunlight intensity of 1000 W/m^2 and a temperature of 25 °C.

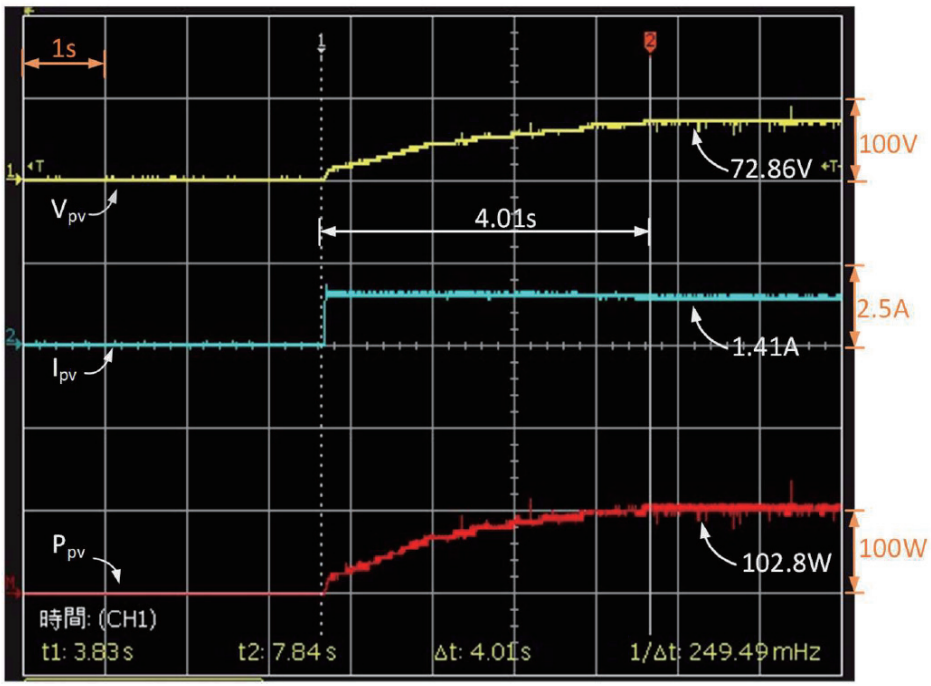

Fig. 15. (Color online) Actual test results of MPPT using the traditional P&O method under a sunlight intensity of 500 W/m^2 and a temperature of 25 °C.

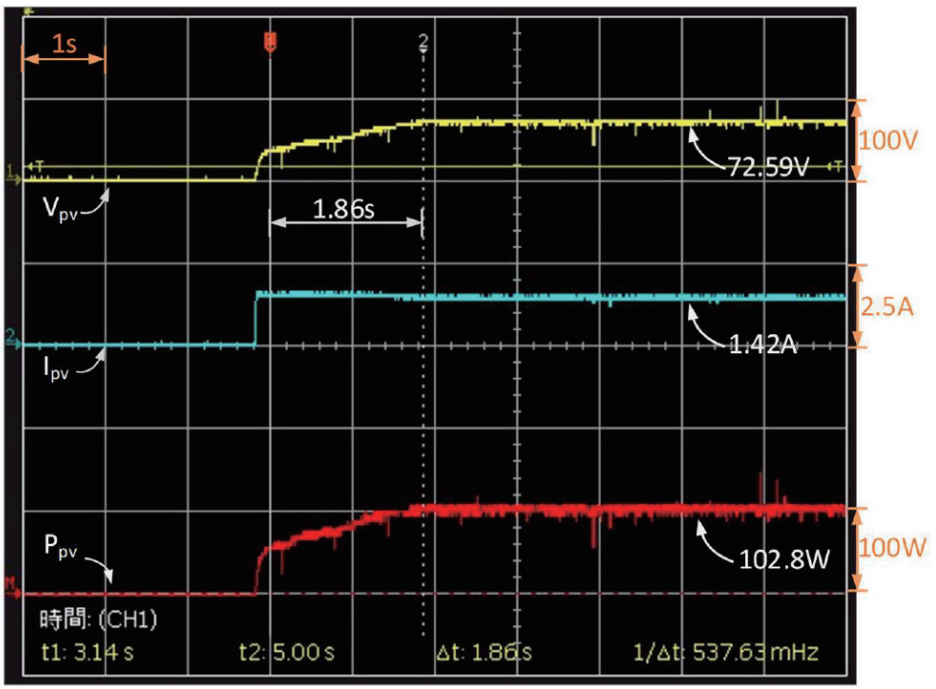

Fig. 16. (Color online) Actual test results of MPPT using the I-P&O method with fixed initial tracking voltage under a sunlight intensity of 500 W/m^2 and a temperature of 25 °C.

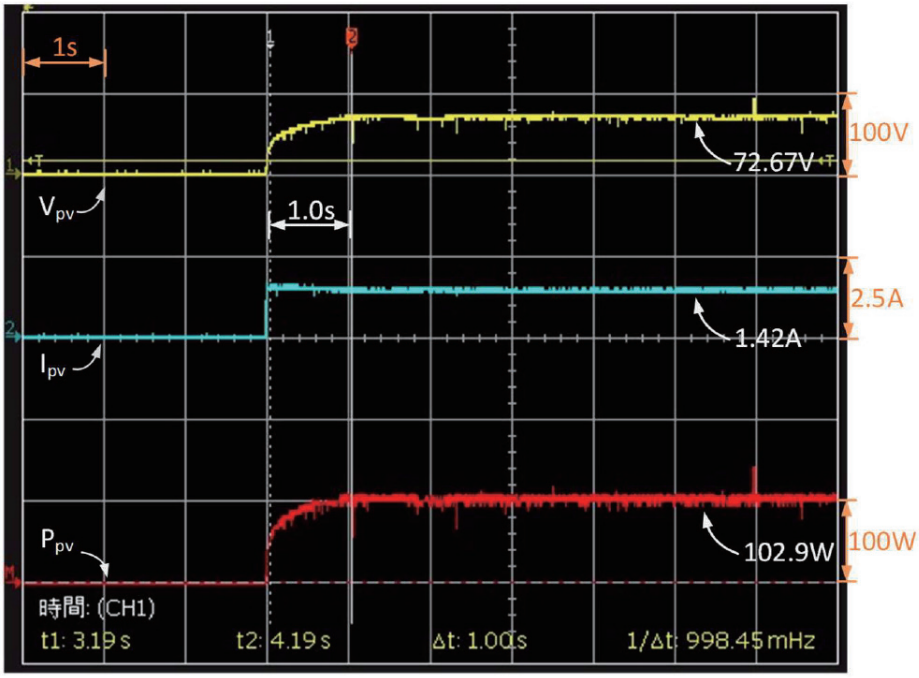

Fig. 17. (Color online) Actual test result of MPPT using the I-P&O method with both fixed initial tracking voltages and step-size adjustment under a sunlight intensity of 500 W/m^2 and a temperature of 25 °C.

It is shown from the actual test results that under a sunlight intensity of 1000 W/m^2, all three tracking methods can track to the MPP of 205 W, MPP voltage of 81 V, and MPP current of 2.5 A. However, the time needed to track to the MPP using the traditional P&O method is 2.99 s, whereas if the I-P&O method with fixed initial tracking voltage is adopted to track to the MPP, the tracking time is only 1.92 s, and if the I-P&O method with both fixed initial tracking voltage and step-size adjustment is used, the tracking time is shortened considerably to 0.92 s. Likewise, under a sunlight intensity of 500 W/m^2, all three tracking methods can track to the MPP of 102 W, MPP voltage of 72.5 V, and MPP current of 1.4 A. However, the time to track to the MPP using the traditional P&O method is 4.01 s, that using the I-P&O method with fixed initial tracking voltage is 1.86 s, and that using the I-P&O method with both fixed initial tracking voltage and step-size adjustment is only 1 s. The test results prove that both proposed I-P&O methods require less time to track to the MPP than the traditional P&O method, especially the I-P&O method with both fixed initial tracking voltage and step-size adjustment; it not only has a faster dynamic response, it also has a better steady-state response performance. Thus, using the I-P&O method to carry out the MPPT for the PVMA achieves better power generation efficiency.

6. Conclusion

In this study, we proposed two I-P&O methods to carry out the MPPT for the PVMA to improve tracking performance. By setting the initial tracking voltage of the traditional P&O method to 0.8-fold the MPP voltage of the PVMA under standard test conditions and adjusting the tracking step size according to the slope of the output *P*—*V* curve for the PVMA, we apply

these two I-P&O methods for the actual PVMA to carry out the MPPT. The two I-P&O methods are that with fixed initial tracking voltage and that with both fixed initial tracking voltage and step-size adjustment. Between the two, the I-P&O method with both fixed initial tracking voltage and step-size adjustment has the better tracking dynamic response. The proposed I-P&O method not only achieves a better tracking response speed than the traditional P&O method, but it can also reduce power loss during the tracking process, thereby improving the power generation efficiency. It is proved through actual test results that, when the sunlight intensity changes, carrying out the MPPT by the proposed I-P&O method can achieve a better tracking dynamic response as well as a steady-state response performance.

Acknowledgments

This work was supported by the Ministry of Science and Technology, Taiwan, under Grant no. MOST 110-2221-E-167-007-MY2.

References

1 Q. Gefei and G. Xia: Proc. 2013 2nd International Symposium on Instrumentation and Measurement, Sensor Network and Automation (2013) 447–450. https://doi.org/10.1109/IMSNA.2013.6743312
2 S. Khatoon, Ibraheem, and M. F. Jalil: Proc. 2014 Innovative Applications of Computational Intelligence on Power, Energy and Controls with their impact on Humanity (2014) 452–456. https://doi.org/10.1109/CIPECH.2014.7019127
3 R. A. Mastromauro, M. Liserre, T. Kerekes, and A. Dell'Aquila: IEEE Trans. Ind. Electron. **56** (2009) 4436. https://doi.org/10.1109/TIE.2008.2004383
4 H. Park, J. Son, and D. Rho: 2009 Transmission & Distribution Conference & Exposition: Asia and Pacific (2009) 1. https://doi.org/10.1109/TD-ASIA.2009.5356886
5 M. A. S. Masoum, H. Dehbonei, and E. F. Fuchs: IEEE Trans. Energy Conv. **19** (2004) 652. https://doi.org/10.1109/TEC.2004.832449
6 T. Esram and P. L. Chapman: IEEE Trans. Energy Conv. **22** (2007) 439. https://doi.org/10.1109/TEC.2006.874230
7 N. Femia, D. Granozio, G. Petrone, G. Spagnuolo, and M. Vitelli: IEEE Trans. Aerosp. Electron. Syst. **43** (2007) 934. https://doi.org/10.1109/TAES.2007.4383584
8 F. Liu, S. Duan, B. Liu, and Y. Kang: IEEE Trans. Ind. Electron. **55** (2008) 2622. https://doi.org/10.1109/TIE.2008.920550
9 Kyocera KS20 Solar Panel, Specifications: https://www.ecodirect.com/Kyocera-KS20-Solar-Panel-20-Watt-12-Volt-p/kyocera-ks20.htm (accessed December 2022).
10 D. W. Hart: Introduction to Power Electronics (Pearson Book Company, 2002) 2nd ed.
11 X. S. Guerrero, J. G. Romero, X. C. Carangui, and G. E. Escrivá: Proc. 51st Int. Univ. Power Engin. Conf. (2016) 1–6. https://doi.org/10.1109/UPEC.2016.8114046
12 R. M. Essefi, Pr. M. Souissi, and Pr. H. H. Abdallah: Proc. 5th Int. Ren. Energy Congr. (2014) 1–6. https://doi.org/10.1109/IREC.2014.6826996
13 R. Bayindir, I. Colak, O. Kaplan, and C. Can: Proc. Int. Conf. Power Engin., Energy and Electr. Drives (2011) 1–4. https://doi.org/10.1109/PowerEng.2011.6036532
14 S. I. Go, S. J. Ahn, J. H. Choi, W. W. Jung, S. Y. Yun, and I. K. Song: J. Int. Counc. Electr. Engin. **1** (2011) 446. https://doi.org/10.5370/JICEE.2011.1.4.446
15 S. S. Chauhan, M. A. Ansari, and O. Singh: Proc. 8th Int. Conf. Signal Proc. Integr. Netw. (2021) 259–264. https://doi.org/10.1109/SPIN52536.2021.9566103
16 Chroma ATE Inc.: https://www.chromaate.com/en/product/dc_power_supply_62000h_series_203 (accessed December 2022).
17 J. Wang and T. T. Liu: Proc. Chinese Contr. Decis. Conf. (2018) 3457–3460. https://doi.org/10.1109/CCDC.2018.8407721

About the Authors

Thi Thanh Truc Bau received her B.S. degree in electrical engineering from National Chin-Yi University of Technology, Taichung, Taiwan, in 2022. She is now studying for a master's degree in National Chin-Yi University of Technology, Taichung, Taiwan. Her areas of interest are power electronics and maximum power point tracking for a photovoltaic module array.

Kuei-Hsiang Chao received his B.S. degree in electrical engineering from National Taiwan Institute of Technology, Taipei, Taiwan, in 1988, and his M.S. and Ph.D. degrees in electrical engineering from National Tsing Hua University, Hsinchu, Taiwan, in 1990 and 2000, respectively. He is presently a tenured distinguished professor at the National Chin-Yi University of Technology, Taichung, Taiwan. His areas of interest are computer-based control systems, applications of control theory, renewable energy, and power electronics. Dr. Chao is a life member of the Solar Energy and New Energy Association and a member of the IEEE.